Clock Stability Characterization and Measurement in Telecommunications

Stefano Bregni, *Member, IEEE*

Abstract— Clock stability characterization and measurement for telecommunications pose peculiar issues and requirements. This paper aims to provide an overview on this subject. After briefly recalling the background work, the key features and issues of clock stability characterization and measurement in telecommunications are described. The timing signal reference model and the stability quantities adopted in the new international standards are introduced and the impact of the measurement configuration and of the time error sampling period on their behavior are elucidated. The measurement of clock stability in telecommunications is then addressed, and a standard practical measurement procedure is outlined. Several measurement results are provided to support the concepts expounded with experimental evidence. The results shown have been chosen among those obtained throughout the last three years by testing clocks of digital switching exchanges, clocks for synchronous digital hierarchy (SDH) equipment, and state-of-the-art stand-alone slave clocks for synchronization networks. They thus represent a survey of the actual performance of clocks currently deployed in telecommunications networks.

Index Terms— Clocks, communication systems, digital measurements, measurement standards, phase noise, phase locked loops, synchronization, synchronous digital hierarchy, time domain measurements.

I. INTRODUCTION

NETWORK synchronization deals with the distribution of time and frequency over a network of clocks spread over a wide geographical area. Network synchronization plays a central role in digital telecommunications [1]–[3]. In fact, while transmission equipment based on the plesiochronous digital hierarchy (PDH) [4] does not need to be synchronized, since a bit justification technique (pulse stuffing) allows multiplexing of asynchronous tributaries with substantial frequency offsets [5], digital switching equipment requires to be synchronized in order to avoid slips in the input elastic stores [6], [7]. And while slips do not significantly affect normal phone conversations, they may be troublesome on some data services. The introduction of circuit-switched data networks and of new advanced services such as those provided by the emerging integrated services digital network (ISDN) created the need of more stringent synchronization requirements. The ongoing spread of SDH technology [8] in transmission networks has made synchronization an important topic in standards bodies in

the last few years: SDH may rely on network synchronization to meet all its performance objectives.

Thus, completely new synchronization standards have been drafted by the International Telecommunication Union Telecommunication Sector (ITU-T) [9]–[11] and by the European Telecommunication Standard Institute (ETSI) [12] following the approach adopted first by the American National Standard Institute (ANSI) [13]. A major topic of discussion in standards bodies has been clock stability characterization and measurement. Based on the previous work and experience, suitable quantities to characterize and specify the stability of telecommunications clocks have been identified and defined in standards documents, together with guidelines for their practical measurement. Several techniques in time and frequency measurement are well-known, but clock stability measurement in telecommunications poses special problems and requirements.

II. BACKGROUND AND FURTHER READING

The literature on time and frequency measurement is extensive and wide-ranging and only the highlights important to the subject of this paper are reviewed here.

The creation of the first cesium-beam clock was in 1955, and by the mid-1960's the need for a common set of frequency-stability-characterization parameters had become extremely important to allow meaningful comparisons between different measurements and performance assessment in terms of the measured data. The resulting pressure to achieve greater uniformity led the IEEE to convene a committee to recommend uniform measures of frequency stability [14], [15].

Since the 1960's, several quantities have been defined to characterize clock stability [16]–[22]. With different characteristics, they highlight distinct phenomena in phase noise or are oriented toward a specific application. A dichotomy developed between stability quantities in the *Fourier frequency domain* (such as power spectral densities of phase and frequency fluctuations) and in the *time domain* (such as variances of the fluctuations averaged over an observation interval). The inadequacy of measurement equipment strengthened the barriers between these two characterizations of the same noise processes. Although these barriers are mainly artificial, it is not always possible to translate unambiguously from a quantity of one domain to one of the other.

In the last 30 years, several experimental test setups have been developed to measure the stability of oscillators in both time and frequency domains [17], [23]–[32]. While measurement techniques in the frequency domain have been

the most common in the past, based on very low-noise analog electronics (e.g., Schottky barrier diodes, analog spectrum analyzers, etc.), recently the availability of high-resolution digital time counters has allowed the time–domain measurement to be more widely used, in telecommunications for example.

Based on this background, suitable quantities for characterizing and specifying the stability of telecommunications clocks have been identified and defined in standards bodies.

III. REFERENCE MODEL OF THE CLOCK TIMING SIGNAL AND BASIC QUANTITIES

In telecommunications, a *clock* is a device able to supply a timing signal, ideally periodic, usable for the control of telecommunications systems. A general expression describing a pseudoperiodic waveform which models the timing signal $s(t)$ at the output of the clock is given by [14] and [22] as

$$s(t) = A \sin \Phi(t) \qquad (1)$$

where A is the peak amplitude and $\Phi(t)$ is the *total instantaneous phase*, expressing the ideal linear increase with t with any frequency drift or random phase fluctuation. The *total instantaneous frequency* is then expressed as

$$\nu(t) = \frac{1}{2\pi} \frac{d\Phi(t)}{dt}. \qquad (2)$$

A common model used to characterize $\nu(t)$ in telecommunications is given by

$$\nu(t) = \nu_{\text{nom}} + \Delta\nu + D\nu_{\text{nom}}t + \frac{1}{2\pi} \frac{d\varphi(t)}{dt} \qquad (3)$$

where $\Delta\nu$ represents the *frequency offset* from the nominal value ν_{nom}, D is the *linear fractional frequency drift* rate, mainly describing oscillator aging effects, $\dot{\varphi}(t)/(2\pi)$ and $\varphi(t)$ [to be not confused with $\Phi(t)$] are, respectively, the *random frequency deviation* and the *random phase deviation,* modeling oscillator intrinsic phase noise sources.

Two functions strictly related to $\dot{\varphi}(t)$ and $\varphi(t)$ are used in treating random frequency and time fluctuations: the *random fractional frequency deviation* $y(t)$ and the *random time deviation*[1] $x(t)$, defined as

$$y(t) = \frac{1}{2\pi\nu_{\text{nom}}} \frac{d\varphi(t)}{dt}, \; x(t) = \frac{\varphi(t)}{2\pi\nu_{\text{nom}}}. \qquad (4)$$

These models and definitions have been widely adopted by specialists since the 1960's [14], [15]. More recently, a need has arisen in telecommunications for the design of synchronization equipment and networks; this has led to the introduction of the following functions which address the timing aspects of clocks.

The *Time* function $\mathrm{T}(t)$ generated by a clock is defined in terms of its total instantaneous phase, as

$$\mathrm{T}(t) = \frac{\Phi(t)}{2\pi\nu_{\text{nom}}}. \qquad (5)$$

[1] Random time deviation should be not confused with the TDEV stability quantity introduced later in Section IV-B.

It is worth noting that for an ideal clock, $T_{id}(t) = t$ holds, as expected. For a given clock, the *Time Error* function $\mathrm{TE}(t)$ between its time $\mathrm{T}(t)$ and a reference time $\mathrm{T}_{\text{ref}}(t)$ is defined as

$$\mathrm{TE}(t) = \mathrm{T}(t) - \mathrm{T}_{\text{ref}}(t). \qquad (6)$$

The time error variation over an interval of duration τ starting at time t (i.e., the error committed by the clock in measuring an interval τ with respect to the reference clock) is called *Time Interval Error* $\mathrm{TIE}_t(\tau)$ and is defined as

$$\mathrm{TIE}_t(\tau) = [\mathrm{T}(t+\tau) - \mathrm{T}(t)] - [\mathrm{T}_{\text{ref}}(t+\tau) - \mathrm{T}_{\text{ref}}(t)]$$
$$= \mathrm{TE}(t+\tau) - \mathrm{TE}(t). \qquad (7)$$

Note that $x(t)$ and $\mathrm{TE}(t)$ have very similar definitions, but differ in that the $\mathrm{TE}(t)$ function takes into account both deterministic [the $\Delta\nu$ and D terms in (3)] and random phase noise components, while $x(t)$ depends on random components only. Isolating the deterministic components in the TE measured data may not be straightforward, and the result can be highly dependent on the parameter estimation technique adopted [24], [25], [33].

IV. CHARACTERIZATION OF CLOCK STABILITY

The random processes $\varphi(t)$, $x(t)$, and $y(t)$ can be characterized in both the frequency and time domains. In the frequency domain, they are commonly characterized in terms of their one-sided power spectral densities (PSD) $\mathrm{S}_\varphi(f)$, $\mathrm{S}_x(f)$, $S_y(f)$, functions of the Fourier frequency f. As mentioned in Section II, the analog measurement of PSD's has long been the main technique for studying the behavior of oscillators. In the time domain, on the other hand, PSD's are commonly characterized for example by variances (e.g., the Allan variance) averaged over an observation interval τ (time).

A. Common Types of Clock Noise

The model most commonly used to represent the phase noise of clocks in the frequency domain is the so-called *power-law model* [22]. In terms of the PSD of $x(t)$ such a model is expressed by

$$S_x(f) = \begin{cases} \dfrac{1}{(2\pi)^2} \displaystyle\sum_{\alpha=-4}^{0} h_{\alpha+2} f^\alpha & 0 \le f \le f_h \\ 0 & f > f_h \end{cases} \qquad (8)$$

where the h_{-2}, h_{-1}, h_0, h_{+1} and h_{+2} coefficients are device-dependent parameters[2] and f_h is an upper cutoff frequency, mainly depending on low-pass filtering in the oscillator and in its output buffer amplifier.[3] This clock upper cutoff frequency

[2] The reason for the subscript $\alpha + 2$ is that, historically, the coefficients h_{-2}, h_{-1}, h_0, h_{+1}, and h_{+2} have been used in the definition of the power-law model in terms of $S_y(f)$. The relationship $S_y(f) = (2\pi f)^2 S_x(f)$ holds [22].

[3] The clock stability measurement setup introduces a further low-pass filtering of the clock output noise, with cutoff frequency $\hat{f}_h$. The actual bandwidth of the $x(t)$ process measured (i.e., the data collected) is therefore limited by the smaller value between f_h and $\hat{f}_h$. Nevertheless, the measurement hardware bandwidth $\hat{f}_h$ of modern stability measurement setups based on digital measurement of the TE (see Section VI-C) is in the range of megahertz and above: this fact ensures usually that all the clock phase noise components are fully considered in performing such measurements.

is usually in the range from 10 to 100 kHz in precision frequency sources [34].

The noise types of this model are white phase modulation (WPM) for $\alpha = 0$; flicker phase modulation (FPM) for $\alpha = -1$; white frequency modulation (WFM) for $\alpha = -2$; flicker frequency modulation (FFM) for $\alpha = -3$; and random walk frequency modulation (RWFM) for $\alpha = -4$. These noise processes may be due to different causes [24]; for some of them, however, the physical bases are not yet fully understood.

The WPM noise, in particular, has little to do with the physical resonance mechanism but is added mainly by noisy electronics. For this reason, in the past it was very seldom recognized in the results of measurements on precision oscillators. Now it is often the most evident noise component in the experimental results measured in telecommunication applications. In fact, modern telecommunication clocks are often based on digitally controlled electronics such as digital phase-locked loops (DPLL) [35]. These produce a quantization error (cf., the measurement results in Section VII-C and Figs. 11–13) appearing as broadband white noise. Similarly, WPM is the background noise caused by the trigger and quantization errors of time counters in the digital measurement of TE (cf., the measurement results in Section VII-A and Figs. 7 and 8).

Though the power-law model proved very general and suitable for describing most measurement results, other types of noise may result in experimental measurements. Periodic noises may be quite common (cf., the measurement results in Section VII-B and Figs. 9 and 10): they are typically caused by 50/60 Hz ac power line interference, diurnal temperature variations, or sensitivity to acoustic or mechanical vibrations, but they may also be caused by intrinsic phenomena such as special frequency control algorithms in DPLL's (cf., the measurement results in Section VII-C and Figs. 11–13).

B. Standard Estimators of the Time–Domain Stability Quantities

While the frequency–domain characterization proves to be very meaningful and complete in studying the behavior of oscillators, it is important to point out that the main concern in digital network synchronization lies in controlling *time* deviations, which impact on the slip rate in elastic stores and on the pointer adjustment rate in SDH nodes. Therefore, the time–domain stability quantities, basically a prediction of the expected time and frequency deviations over an observation interval, are more relevant to this field.

This issue and the availability of digital time counters of increasing resolution have made the time–domain stability quantities and measurement techniques the standard choice in telecommunications. As will be demonstrated, these techniques basically consist of measuring a sampled version of the process TE(t) and then computing all the stability quantities of interest based on the acquired data sequence.

Thus, among the several quantities defined in the literature to characterize time and frequency stability, the following five time-domain quantities have been considered by international telecommunication standards bodies [9], [12] for the specification of timing-interface requirements: the *Allan*

deviation (ADEV), i.e., the square root of the Allan variance (AVAR); the *modified Allan deviation* (MADEV), i.e., the square root of the modified Allan variance (MAVAR); the *time deviation* (TDEV), i.e. the square root of the time variance (TVAR); the *root mean square of time interval error* (TIErms); and the *maximum time interval error* (MTIE). As far as the formal definition of the first three quantities and the relevant theoretical background are concerned, the reader is referred to [14] and [16]–[21]. The last two quantities, on the other hand, have been introduced mainly by telecommunications engineers and may appear somehow "exotic" to the traditional world of time and frequency metrology; a detailed analysis of their properties is available in [36] and [37].

While TIErms and MTIE have been defined based on the TE process, ADEV, MADEV, and TDEV are theoretically defined in terms of the $x(t)$ process of (4), i.e., the random time deviation stripped of the deterministic components. Nevertheless, in order to overcome the complex problem of removing the frequency offset and drift from the TE measured data—and to achieve uniformity in the evaluation procedure of all the five standard stability quantities—the international telecommunication standards bodies simply recommend the use of TE(t) samples instead of $x(t)$ samples also for ADEV, MADEV, and TDEV measurements. This choice is well-justified based on the following:

- ADEV, MADEV, and TDEV are not sensitive to any linear frequency offset in the TE data (they are based on a second difference operator, analogous in the discrete-time domain to the second derivative in the continuous-time domain);
- the frequency drift contribution is usually negligible in the observation intervals of interest in telecommunications ($\tau < 10^4$ s);
- the concern is not to rigorously characterize the noise types affecting the clock under test, but simply to limit the overall time deviations for the purposes of network design.

According to the above statements, from now on, for the purposes of telecommunication clock stability measurement, we shall consider the processes TE(t) and $x(t)$ synonymous and refer to the time error samples TE(t_i) simply as $x(t_i)$. Therefore, based on a sequence of N TE samples, defined as

$$x_i = x[t_0 + (i-1)\tau_0] \qquad i = 1, 2, \cdots, N \qquad (9)$$

where τ_0 is the sampling period used in the measurement interval $T = (N-1)\tau_0$ starting at time t_0, the five standard estimators [as shown in (10)–(14) at the bottom of the next page] have been defined by the ITU-T [9] and ETSI [12] bodies where $\tau = n\tau_0$ is the so-called *observation interval* and $\lfloor z \rfloor$ denotes *"the greatest integer not exceeding z"*. Until now, mainly MTIE and TDEV have been used in standard specifications.

V. BEHAVIOR OF THE STABILITY QUANTITIES

All the above frequency stability quantities are sensitive, in various ways, to the presence of the noise types in the timing signal mentioned in Section IV-A [24], [36]. It is widely
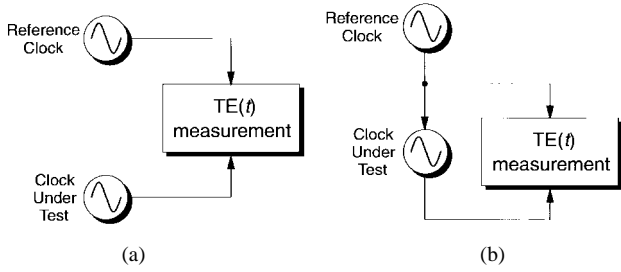
Fig. 1. ITU-T and ETSI standard measurement configurations on a single clock.

Fig. 2. Comparison of ADEV curves computed (theoretical model) in the independent and synchronized clocks configurations ($b = 1$ Hz).

known, for example, that the dependence of the slopes of the ADEV, MADEV, TDEV, and TIErms curves on the different types of power-law noise (8), while periodic noise appears in the plots of the time-domain stability quantities as a ripple (cf., the measurement results in Section VII-B and VII-C and Figs. 9–13). The reader is referred to the cited works for further details on these topics.

Two key issues are the impact of the measurement configuration and of the TE sampling period on the trends of the stability quantities. These issues must be considered when performing stability measurement in order to draw meaningful conclusions from the measurement data.

A. Impact of the Measurement Configuration

As far as the characterization of the stability of a single clock is concerned, two measurement configurations have been defined by the international telecommunication standards bodies ITU-T and ETSI [9], [12]. In the *independent clocks configuration* [see Fig. 1(a)], the reference time $T_{ref}(t)$ of (6) is the time generated by a second independent clock, usually a highly accurate and stable one such as an atomic frequency standard. In the *synchronized clocks configuration* [see Fig. 1(b)], $T_{ref}(t)$ is the input to a slave clock, while $T(t)$ is its output.
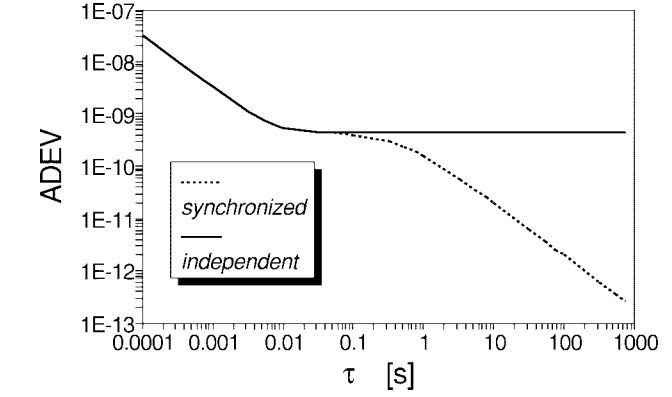
The measurement configuration substantially affects the behavior of the stability quantities. As shown in [36] and [38], the noise generated by the internal oscillator of the slave clock, implemented as a phase-locked loop (PLL), is high-pass filtered by the closed loop to the output, so that the curves of the stability quantities, measured in the two configurations, match in the short term (i.e., for $\tau \ll 1/2\pi B$, where B is the bandwidth of the closed-loop filter), but they exhibit a substantially different trend for any longer τ. More detailed information on the asymptotic trends of the stability quantities in both measurement configurations can be found in [36]. As a sample case, Fig. 2 shows two ADEV curves, numerically computed for the two configurations with $B = 1$ Hz. Measurement results shown in Section VII-D and Fig. 14 confirm the same trends.

B. Impact of the TE Sampling Period

The choice of the TE sampling period τ_0 implies a tradeoff between the resolution and the duration of the measurement: for a fixed number of samples N, the shorter τ_0 the shorter is the minimum observation interval τ, the longer τ_0 the longer is

$$\text{ADEV}(\tau) = \sqrt{\frac{1}{2n^2\tau_0^2(N-2n)} \sum_{i=1}^{N-2n} (x_{i+2n} - 2x_{i+n} + x_i)^2} \qquad n = 1, 2, \cdots, \left\lfloor \frac{N-1}{2} \right\rfloor \tag{10}$$

$$\text{MADEV}(\tau) = \sqrt{\frac{1}{2n^4\tau_0^2(N-3n+1)} \sum_{j=1}^{N-3n+1} \left[\sum_{i=j}^{n+j-1} (x_{i+2n} - 2x_{i+n} + x_i) \right]^2} \qquad n = 1, 2, \cdots, \left\lfloor \frac{N}{3} \right\rfloor \tag{11}$$

$$\text{TDEV}(\tau) = \frac{\tau}{\sqrt{3}} \text{MADEV}(\tau) =$$

$$\sqrt{\frac{1}{6n^2(N-3n+1)} \sum_{j=1}^{N-3n+1} \left[\sum_{i=j}^{n+j-1} (x_{i+2n} - 2x_{i+n} + x_i) \right]^2} \qquad n = 1, 2, \cdots, \left\lfloor \frac{N}{3} \right\rfloor \tag{12}$$

$$\text{TIErms}(\tau) = \sqrt{\frac{1}{N-n} \sum_{i=1}^{N-n} (x_{i+n} - x_i)^2} \qquad n = 1, 2, \cdots, N-1 \tag{13}$$

$$\text{MTIE}(\tau) = \max_{1 \le k \le N-n} \left[\max_{k \le i \le k+n} x_i - \min_{k \le i \le k+n} x_i \right] \qquad n = 1, 2, \cdots, N-1 \tag{14}$$

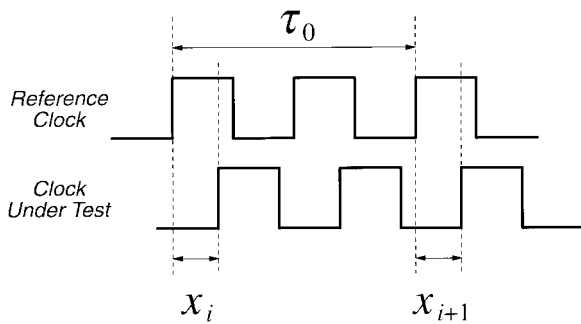Fig. 3.   TE measurement and sampling on square-wave timing signals.

Fig. 4.   Taxonomy of time and frequency measurement techniques.

the maximum τ. In practical applications, τ might even range from 10^{-3} s up to 10^6 s, thus yielding the choice $\tau_0 = 10^{-3}$ s, if aiming at characterizing the overall behavior of the stability quantities on such a whole range of τ. In order to overcome the storage and processing of billions of samples, one might operate on subranges of the whole range of τ as follows:

1) for each subrange, choose τ_0 equal to the minimum τ of the subrange and collect measurement data;
2) for each subrange, evaluate the stability quantities based on the TE data collected;
3) *juxtapose* the resulting curves.

Unfortunately, it may be shown [39] that, while ADEV, MTIE, and TIErms do not feature any significantly different behavior as the sampling period is varied for the power-law noise types of (8), the behavior of MADEV and TDEV is substantially dependent on the chosen measurement sampling period in the observation intervals where WPM or FPM noises dominate. In such a case, the above procedure fails when juxtaposing the curves of different subranges (extremes do not meet). Some measurement results confirming this potential trouble are shown in Section VII-E and Fig. 15. As a final remark, it is worthwhile noting that MTIE may also exhibit some slight dependence on the TE sampling period. This issue is discussed in [37] and [39].

VI. MEASUREMENT OF TELECOMMUNICATIONS CLOCK STABILITY

As discussed in Section II, several measurement techniques have been developed to measure the stability of precision oscillators. Though most of them were conceived when digital instrumentation was not yet available (e.g., for spectrum analog measurement), nowadays they are mainly considered to enhance the sensitivity of digital time counters for time–domain measurements.

A. Taxonomy of Time and Frequency Measurement Techniques

The most straightforward method is to measure directly the time error by means of a digital time counter (*direct digital measurement of time error*), triggered by the zero-crossings of the timing signals generated by the clock under test (CUT) and the reference clock (RC), as shown in Fig. 3 for two clock square waves.

Even though the resolution of modern digital time counters is continuously improving (typically from 20 to 200 ps),
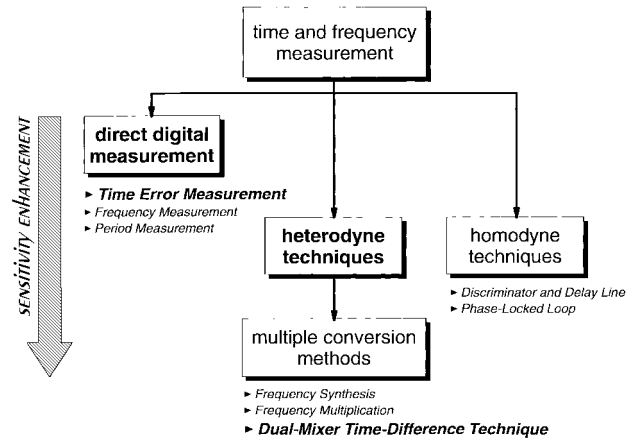
the short-term time fluctuations of a state-of-the-art crystal oscillator may be even smaller, up to the order of 1 ps. (Do not let *resolution* be confused with *precision*: the actual precision of any instrumentation has manifestly nothing to do with the number of digits displayed!) Therefore, several sensitivity-enhancement methods have been developed, aiming at distinguishing very small time and frequency fluctuations. These methods can be classified as follows:

- *heterodyne techniques* (from the Greek etyma $\overset{'}{\epsilon}\tau\epsilon\rho o\varsigma = different$ and $\delta v\nu\alpha\mu\iota\varsigma = force$), which consist of mixing (i.e., multiplying in the time domain) the timing signal under test with the reference signal, at *almost* the same frequency, to measure the same *phase* fluctuations but at the resulting low-frequency beat signal (thus measuring larger *time* fluctuations);
- *homodyne techniques* (from the Greek etymon $\overset{'}{o}\mu o\varsigma = same$), which are a limit of the previous method, occurring when the mixed reference signal has the *same* average frequency of the signal under test (the reference signal is obtained from the signal under test for example by means of a phase-locked loop (PLL) or a delay line);
- *multiple conversion techniques*, in which the actual signal to measure is obtained from the signal under test through several mixing and frequency synthesis stages; among them, the dual-mixer time-difference (DMTD) technique may be considered the current state of the art of time and frequency stability measurements.

All the above techniques are discussed in detail in the cited works (good general surveys are provided particularly by [23]–[25]). The taxonomy of the main time and frequency measurement techniques is summarized in Fig. 4, where the methods most relevant to telecommunications applications are highlighted in boldface, as discussed in the following section.

B. Distinctive Features of Clock Stability Measurement in Telecommunications

Time and frequency stability measurements are used in telecommunications mainly for three different purposes:

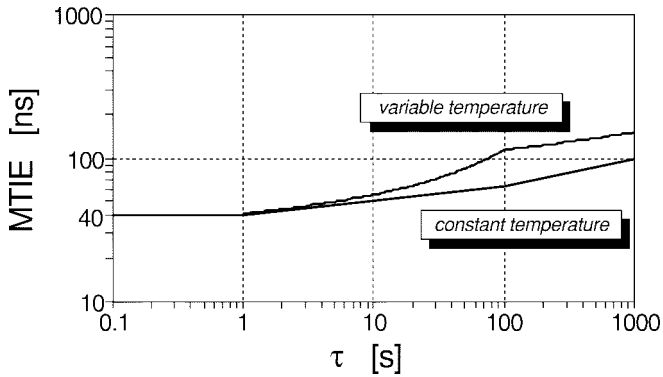1) *conformance testing* of clocks, i.e., for simply checking their compliance to relevant standards;

Fig. 5. MTIE mask for SEC (option 1) wander generation specified in ITU-T Rec. G.813.

2) *performance evaluation*, aiming at a deeper insight into the actual clock behavior and noise characterization;

3) *in-service performance monitoring* of timing equipment deployed in offices, to ensure proper operation of the whole telecommunications network, by means of field personnel or built-in hardware.

Aside from the purpose, clock stability measurement in telecommunications poses peculiar issues with respect to traditional laboratory measurements on simple oscillators. Its most distinctive features may be summarized as follows.

- The range of interest of the observation interval τ is usually centered on the range 10^{-1}s $\leq \tau \leq 10^4$ s, over which the international standards specify the limit values of MTIE and TDEV stability quantities.

- Several state-of-the-art, stand-alone, and equipment clocks (as in the case of DPLL's), though built around a very low-noise crystal or atomic oscillator, control the output frequency by means of digital electronics and numerical algorithms. These may produce a considerable short-term noise of amplitude, in some cases up to *tens* of nanoseconds, in the output timing signal (cf., the measurement results in Section VII-C and Figs. 11–13).

- The standard masks (i.e., the graph plots of the allowed limits) specifying telecommunications clock stability [10], [12] allow rather high noise limits, well above the resolution of the currently available time counters. As an example, Fig. 5 depicts one of the ITU-T G.813 MTIE masks [10], specifying the stability of SDH equipment clocks (SEC's) in terms of peak-to-peak TE under both constant and variable temperature conditions.

- Time and frequency measurements in telecommunications applications do not necessarily take place in a laboratory under strictly controlled conditions, but often are accomplished in the field.

All the above features make the TE direct digital measurement well-suited to telecommunications clock stability testing, though not adequate to resolve the short-term time fluctuations of state-of-the-art oscillators (i.e., for $\tau \ll 1$ s). On one hand, the resolution of a good time counter (of the order of 200 ps or less) is perfectly suitable for measuring the stability of most telecommunications clocks in the range of interest 10^{-1}s $\leq \tau \leq 10^4$ s, also beyond mere conformance testing. On the other
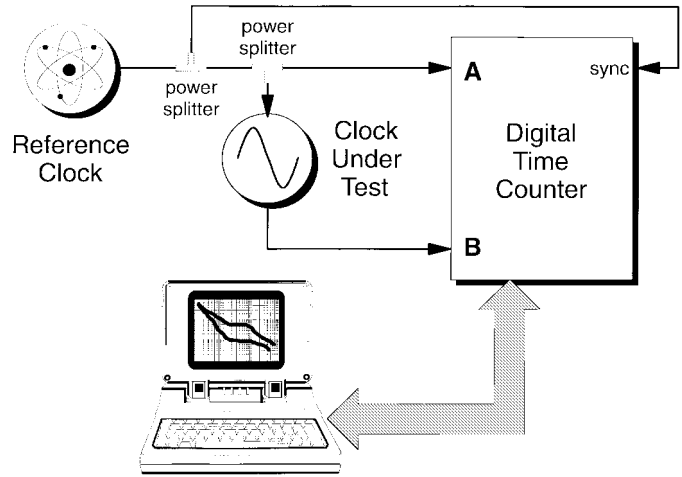

Fig. 6. Measurement setup for TE acquisition, storing, and post-processing (synchronized clocks configuration).

hand, the robustness of this setup is essential when performing field-measurements, where more sophisticated sensitivity-enhancement methods may more easily suffer mechanical or electromagnetic interferences. The only measurements which may require the sensitivity-enhancement power of heterodyne or DMTD techniques is the performance evaluation in the short term (τ in the range from 1 ms to 1 s) of very low-noise state-of-the-art clocks.

C. Practical Measurement Procedure

According to what was stated in the previous sections, the following practical measurement procedure has been consolidated as a standard to assess the stability of telecommunication clocks, also beyond mere conformance testing.

1) TE Data Acquisition:

> Acquire and store a sequence $\{x_i\}$ of N samples of TE, with sampling period τ_0 and over a measurement interval $T = (N - 1)\tau_0$.

Typical values of the measurement parameters are τ_0 in the order of a few milliseconds and T up to 10^3–10^4 s. Latest ITU-T standards [10] recommend $\tau_0 \leq 33$ ms and $T \geq 12\tau$. Moreover, they recommend to measure the data, for observation intervals in the range from 0.1 s to 1000 s, "*through an equivalent 10 Hz, first-order, low-pass measurement filter*." The rationale of this choice has been the wish of getting rid of the spectrum aliasing which may occur by subsampling the TE function in the presence of broadband noise. Nevertheless, in the opinion of the author of this paper, this is questionable [40] and might be amended before the final approval of the standards. Actually, being that such standards are still drafts and subject to further revisions, the engineer carrying out these measurements is encouraged to check the latest version of the standards for all the details.

The samples x_i are usually collected through direct digital measurement of the TE between the CUT and the RC, as shown in Fig. 3 for two clock square waves. A typical test setup is shown in Fig. 6 for the case of the synchronized

clock configuration. The RC (an atomic frequency standard is a good choice, especially when performing measurements in the independent clocks configuration) should also supply the time base to the time counter. Data acquisition, storing and subsequent post-processing are accomplished by a computer interfaced to the time counter.

When special sensitivity is required, e.g., for laboratory characterization of the short-term noise of very good clocks, TE measurement may be alternatively accomplished through more sophisticated methods, such as heterodyne or DMTD techniques.

2) Numerical Post-Processing:

> Compute the stability quantities of interest (viz. ADEV, MADEV, TDEV, MTIE, TIErms) with the standard estimators of (10)–(14) based on the acquired sequence $\{x_i\}$.

Other meaningful quantities (e.g., PSD's, autocovariance function, other variances, etc.) may be computed as well with suitable numerical algorithms [41]. Moreover, it is worth noting that MTIE computation in most practical cases may be quite difficult and troublesome, owing to its distinctive nature of peak measurement and to the number of operations nested in the estimator (14). This issue is discussed in [37].

3) Background Noise Floor Measurement:

> Do the same without the CUT shown in Fig. 6, by directly feeding the RC timing signal split into the time counter input ports, for assessing the background noise floor of the test setup of the previous measurement.

This step is very important in discriminating which measurement results are really due to the CUT and which are added by instrumentation: a quick comparison of the stability curves obtained in the two cases allows the assessment of where the clock noise was measured and where the test equipment noise dominates instead.

VII. MEASUREMENT RESULTS

The measurement procedure outlined in Section VI-C has been extensively applied throughout the last years in testing several telecommunications clocks, for conformance testing, and for research purposes, within the national activities for the development of the new Italian synchronization network. This section provides a broad selection of measurements results in order to support the concepts expounded in the previous sections with experimental evidence. Additional measurement results on SDH equipment clocks can be found in [42] and several MTIE measurement results on clocks of various types are featured by [37].

All the results shown (except those in Section VII-D) were measured in the synchronized-clock configuration, according to Figs. 3 and 6. A digital time counter, with a resolution of 200 ps, measured the TE between the output timing signal of the CUT and its input reference (both G.703§10 [5] signals at 2.048 MHz unless otherwise stated). The latter was synthesized from the 10 MHz output signal of the RC, a rubidium frequency standard, which also supplied the time base to the time counter. The time counter was driven by a laptop computer via a GPIB IEEE488.2 interface which controlled data acquisition and then accomplished numerical processing of the data and the visualization of the results.

The hardware bandwidth of the time counter is on the order of 500 MHz. Moreover, measuring the TE between two 2.048 MHz square signals imposes a maximum bandwidth $\hat{f}_h$ of the measured phase fluctuations not larger than 2.048 MHz. Nevertheless, the natural cutoff frequency f_h (8) of the clock output noise is not expected to be larger than 100 KHz [34]. Since $\hat{f}_h > f_h$, it is then not necessary to specify exactly the actual value of $\hat{f}_h$, as it does not substantially affect the total phase noise power measured (cf., Section IV-A).

Every set of stability curves shown in the following was evaluated basing on a TE sequence of N samples measured with sampling period τ_0 and over a measurement interval T. The ADEV, MADEV, TDEV, TIErms, and MTIE curves were computed for up to 24 points/decade to achieve an excellent rendering of actual trends, with the standard estimators of (10)–(14). Moreover, the PSD $S_x(f)$ was computed (neglecting a multiplicative factor) on 1024 points through the fast Fourier transform (FFT) periodogram technique with Parzen data windowing (triangular shape) [41], while the autocovariance function $C_x(\tau)$ was evaluated (neglecting a multiplicative factor) on 2047 points, as inverse transform of the PSD for $\tau \geq 0$ and mirrored copy for $\tau < 0$.

A. Background WPM Noise Floor of the Measurement Setup

According to what we stated in Section VI-C3, the background noise of the measurement setup was measured by splitting the 2.048 MHz reference timing signal, synthesized from the rubidium oscillator output, and by feeding it directly into the time counter input ports, in order to assess whether the results measured on actual clocks were indeed meaningful or not.

This background noise is mainly caused by the trigger and quantization errors of the time counter and proves a pure WPM broadband noise, as shown by the measurement results provided in Figs. 7 and 8. The ADEV and MADEV curves in Fig. 7 are straight lines with slopes of τ^{-1} and $\tau^{-3/2}$, respectively, in perfect accordance with well-known theory [14], [22], [36], while the autocovariance $C_x(\tau)$ plotted in Fig. 8 for $|\tau| \leq 10$ s features a $\delta(\tau)$ spike[4] at $\tau = 0$.

B. Periodic Noise

An example of periodic noise is provided in Figs. 9 and 10, showing results measured on the SEC of a SDH line terminal multiplexer STM-16 (LTM-16). The PSD in Fig. 9 exhibits

---

[4]The spike has width limited to the central sample $C_x(0)$. For the sake of precision, the first numerical values are $C_x(0) = 6.3 \cdot 10^{-6}$, $C_x(\pm\tau_0) = 6.8 \cdot 10^{-8}$, $C_x(\pm 2\tau_0) = 8.3 \cdot 10^{-8}$, $C_x(\pm 3\tau_0) = 3 \cdot 10^{-8}$, $C_x(\pm 4\tau_0) = 3.2 \cdot 10^{-8}$, $C_x(\pm 5\tau_0) = 1.8 \cdot^{-8}$, etc.
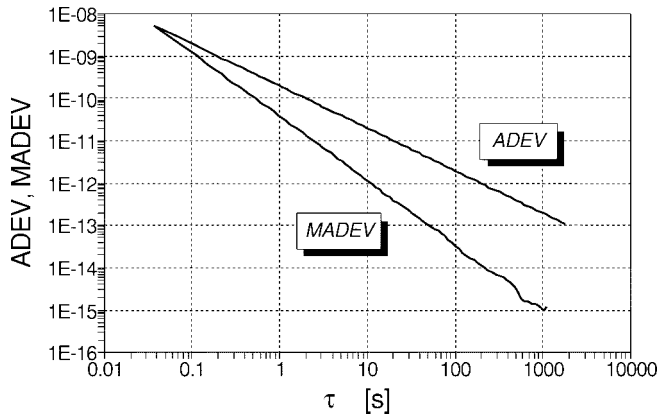
Fig. 7.   Trigger and quantization WPM noise: ADEV (τ) and MADEV (τ) (measurement results, $N = 96\,700$, $\tau_0 \cong 37$ ms, $T = 3600$ s).
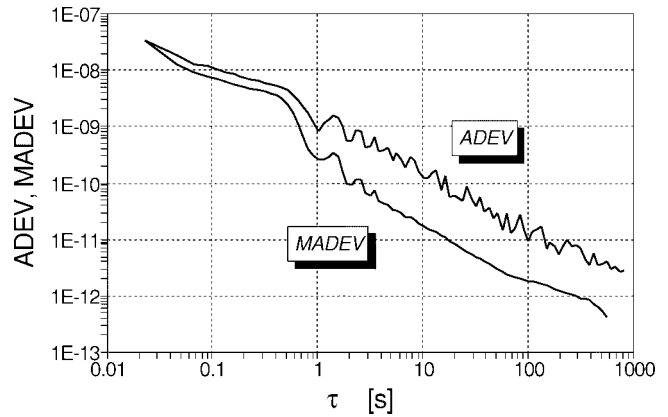

Fig. 10.   Periodic noise measured on a LTM-16 SEC: ADEV(τ) and MADEV(τ) ($N = 79\,000$, $\tau_0 \cong 23$ ms, $T = 1800$ s).
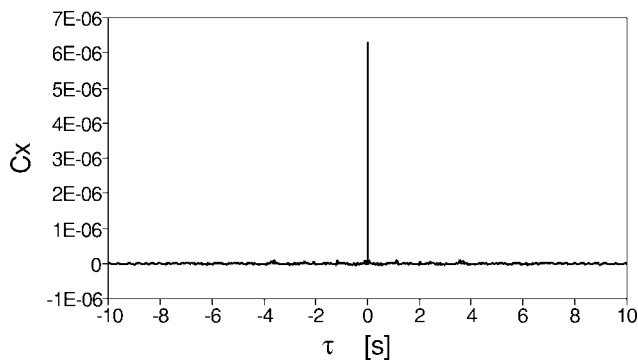

Fig. 8.   Trigger and quantization WPM noise: autocovariance function $C_x(\tau)$ (measurement results, $N = 96\,700$, $\tau_0 \cong 37$ ms, $T = 3600$ s).
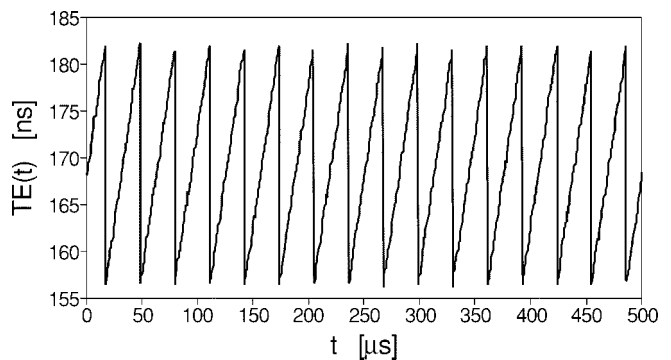

Fig. 11.   Periodic noise measured on an ADM-1 SEC: first quarter of the TE sequence $\{x_i\}$ ($N = 4096$, $\tau_0 \cong 488$ ns, $T = 2$ ms).
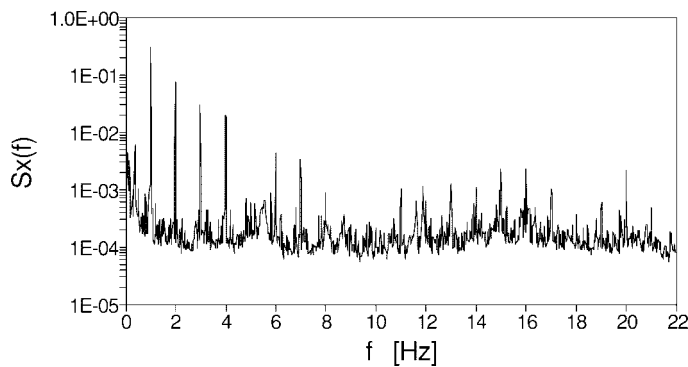
Fig. 9.   Periodic noise measured on a LTM-16 SEC: PSD estimate $S_x(f)$ ($N = 79\,000$, $\tau_0 \cong 23$ ms, T$= 1800$ s).
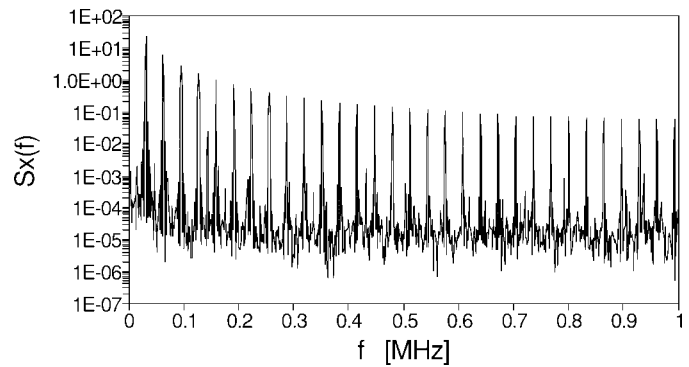

Fig. 12.   Periodic noise measured on an ADM-1 SEC: PSD estimate $S_x(f)$ ($N = 4096$, $\tau_0 \cong 488$ ns, $T = 2$ ms).

several discrete terms (spikes) in the frequency domain, at harmonic frequencies of about 1 Hz. In the time–domain analysis, on the other hand, the same periodic noise appears as a ripple (see the ADEV and MADEV plots in Fig. 10).

C. Yet Another Periodic Noise: Short-Term Quantization Noise in a DPLL

As mentioned in Sections IV-A and VI-B, some DPLL's implement frequency control numerical algorithms producing a substantial short-term noise. This subsection deals with the SEC of an early design of SDH add-drop multiplexer STM-1 (ADM-1). Aiming at studying the clock behavior in the very

short term, the maximum TE sampling rate was set, measuring the TE on *every* edge of the 2.048 MHz timing signals (hence $N = 4096$, $\tau_0 \cong 488$ ns, $T = 2$ ms).

Fig. 11 details the first 500 μs of the acquired TE sequence, which exhibits a saw-toothed waveform of 26 ns peak-to-peak amplitude and of period around 30–40 μs. This plot reveals that this DPLL operates stepping alternatively between two discrete frequencies (frequency quantization error), controlled by a phase threshold mechanism. In this limit case, the PSD (Fig. 12) consists of a series of spikes and the ripples in the ADEV and MADEV plots (Fig. 13) are also very wide. Moreover, it is worth noting that such

a short-term noise, when performing measurements with a long sampling period, appears as a broadband WPM noise.

D. Impact of the Measurement Configuration

The impact of the measurement configuration (cf., Section V-A) on the trends of the stability quantities is well-demonstrated by the measurement results [43] of Fig. 14. The CUT was a state-of-the-art slave clock for synchronization networks, i.e., a stand-alone synchronization equipment (SASE) according to ITU-T and ETSI standard terminology or a building integrated timing supply (BITS) according to ANSI. The SASE, deployed in a public switched telephone network (PSTN) office, was equipped with a quartz oven controlled crystal oscillator (OCXO) and had its bandwidth set to $B = 5$ MHz.

Two sequences were measured: the former in the synchronized clocks configuration and the latter in the independent clocks configuration. The dotted curves in Fig. 14 were evaluated based on the former sequence, while the solid ones were based on the latter. Moreover, the upper two curves depict ADEV results, while the lower two show those of MADEV. These measurement results confirm the theoretical indications of Section V-A: the stability curves, though measured on different days, match approximately in the short term for $\tau \ll 1/2\pi B \cong 30$ s but separate from there on.

E. Impact of the TE Sampling Period

In order to support the conclusions stemming from simulations (Section V-B) with experimental evidence, measurements were carried out on the OCXO clock of a world-wide deployed PSTN digital switching exchange (HDB3-coded G.703§6 [5] timing signals at 2.048 Mb/s). First, a TE sequence ($N = 500\,000$, $\tau_0 \cong 7.5$ ms, $T = 3600$ ms) was acquired and then sample decimation was accomplished, yielding a set of six other sequences, respectively, with sampling periods equal to $2\tau_0 = 15$ ms, $5\tau_0 = 37.5$ ms, $10\tau_0 = 75$ ms, $20\tau_0 = 150$ ms, $50\tau_0 = 375$ ms, $100\tau_0 = 750$ ms, and thus of length $N = 250\,000$, $100\,000$, $50\,000$, $25\,000$, $10\,000$, 5000. Based on these decimated sequences, the TDEV(τ) was evaluated and plotted in the graph shown in Fig. 15.

Here, the slopes of the TDEV curves show the dominant presence in the timing signal under test of WPM and FFM noises. In particular, the WPM noise appears to be dominant for $\tau < 10$ s: for any given observation interval in that region, TDEV(τ) takes increasing values as the sampling period is increased. No such dependence is recognizable for $\tau > 10$ s, where FFM noise dominates instead.

FFM noise is usually not recognizable in measurement results obtained in the synchronized clocks configuration, owing to its low-frequency nature, because the noise generated by the internal oscillator of the slave CUT is high-pass filtered by the closed loop to the output (see Sections V-A and VII-D). In this case, nevertheless, the closed-loop time constant was very high (>100 s) and out of the range of τ under measurement.
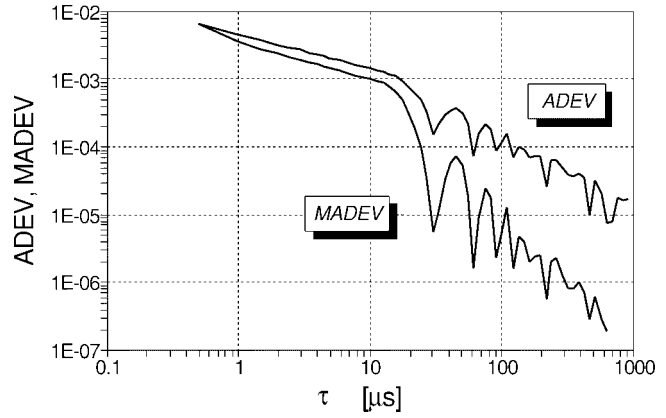

Fig. 13. Periodic noise measured on an ADM-1 SEC: ADEV(τ) and MADEV(τ) ($N = 4096$, $\tau_0 \cong 488$ ns, $T = 2$ ms).
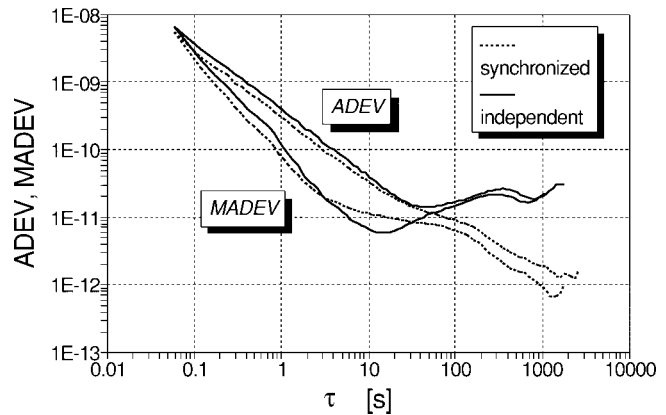

Fig. 14. Comparison of ADEV(τ) and MADEV(τ) curves measured on a SASE in the synchronized ($N = 90\,000$, $\tau_0 \cong 60$ ms, $T = 5400$ s) and independent ($N = 60\,000$, $\tau_0 \cong 60$ ms, $T = 3600$ s) clocks configurations.
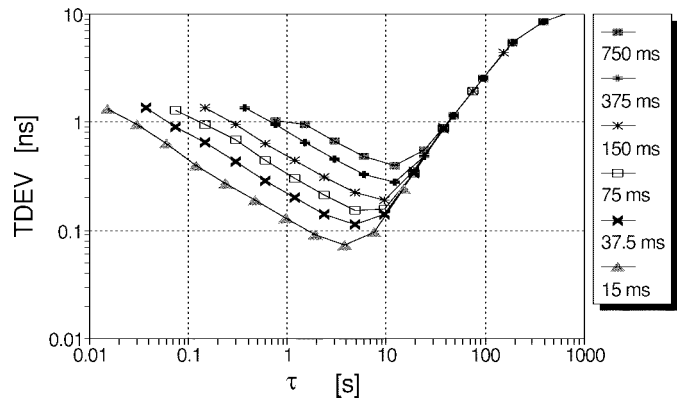

Fig. 15. TDEV(τ) curves measured on a PSTN digital switching exchange clock for different sampling periods ($T = 3600$ s).

F. Final Example of Experimental Clock Characterization

As a final example of experimental clock characterization through the measurement procedure outlined in Section VI-C, this subsection features a complete set of graphs of stability quantities, computed from a sequence measured on the SEC of an ADM-4 of the same supplier as the ADM-1 dealt with in Section VII-C (actually, the ADM-4 clock was designed more
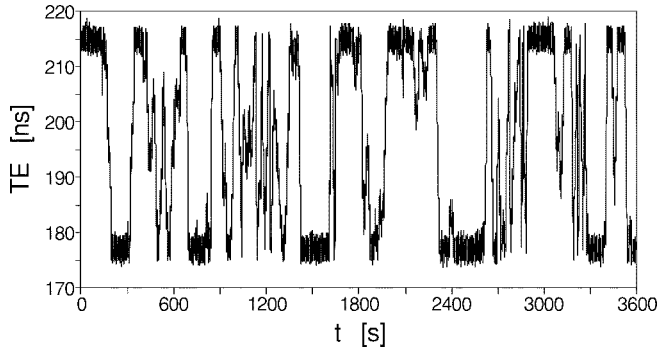
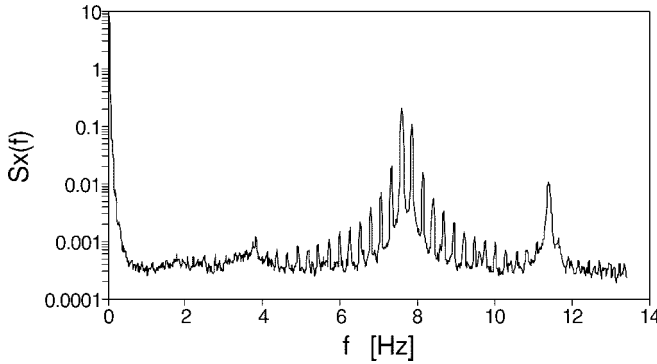Fig. 16. TE sequence $\{x_i\}$ measured on an ADM-4 SEC ($N = 96\,750$, $\tau_0 \cong 37.5$ ms, $T = 3600$ s).

Fig. 17. PSD estimate $S_x(f)$ measured on an ADM-4 SEC ($N = 96\,750$, $\tau_0 \cong 37.5$ ms, $T = 3600$ s).

Fig. 18. ADEV(τ) and MADEV(τ) curves measured on an ADM-4 SEC ($N = 96\,750$, $\tau_0 \cong 37.5$ ms, $T = 3600$ s).

Fig. 19. TDEV(τ) and TIErms(τ) curves measured on an ADM-4 SEC ($N = 96\,750$, $\tau_0 \cong 37.5$ ms, $T = 3600$ s).

Fig. 20. MTIE(τ) curve measured on an ADM-4 SEC ($N = 96\,750$, $\tau_0 \cong 37.5$ ms, $T = 3600$ s).

recently, and it is supposed to be an improved version of the previous model).

The graphs shown in Figs. 16–20 summarize in one experimental example some of the concepts detailed previously.

- Though the DPLL's frequency quantization error of the ADM-1 (the 26 ns short-term saw-toothed noise of Fig. 11) appears to have been eliminated in this new design, a slower wander appears in the TE process of this clock. As shown by the graph in Fig. 16, these TE fluctuations even exceed 45 ns. This pseudoperiodic component does not appear in the PSD of Fig. 17, because of its very low Fourier frequency.
- The PSD in Fig. 17 exhibits several spikes at harmonic frequencies centered around $f_1 = 3.8$ Hz, $f_2 = 7.6$ Hz, $f_3 = 11.4$ Hz. These periodic components appear as ripples in the time domain plots of ADEV, MADEV, TDEV, and TIErms (Figs. 18 and 19).
- The ADEV and MADEV curves in Fig. 18 exhibit the typical inflection point of the measurements in the synchronized clocks configuration (cf., Figs. 2 and 14).
- The MTIE plot of Fig. 20 confirms that the 45 ns output TE shifts of the CUT may be sharp: the MTIE curve rises from 7 to 45 ns in the interval 1 s $\leq \tau \leq$ 10 s.

Finally, it must be pointed out that repeated measurements on this SEC yielded similar results. Therefore, the behavior herein shown is not accidental but should be considered typical of this clock.
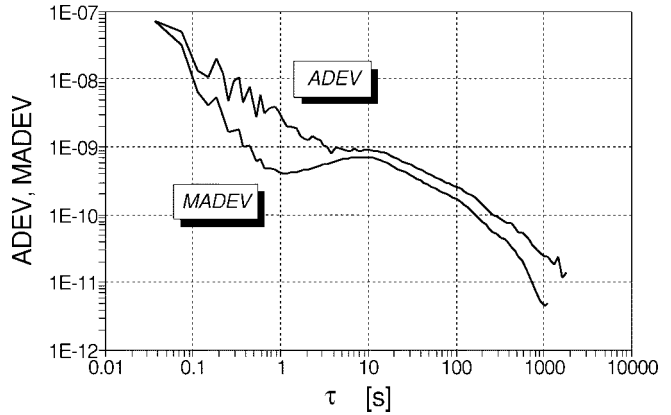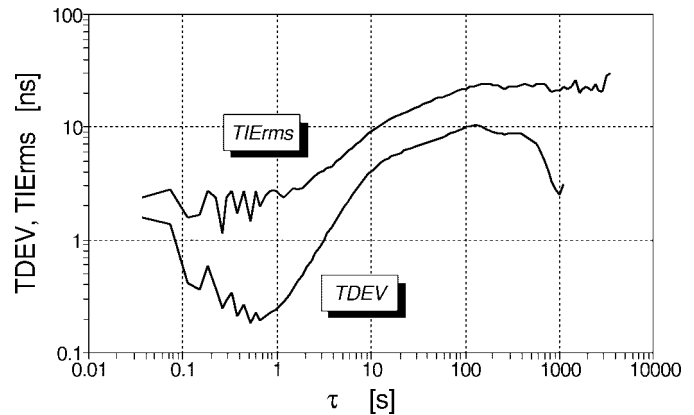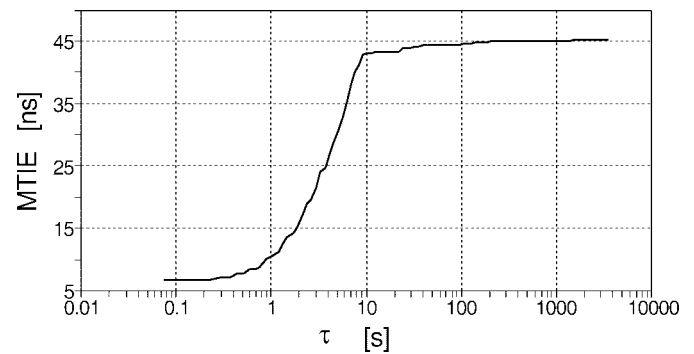
VIII. CONCLUSIONS

The key features and issues of clock stability characterization and measurement in telecommunications have been described pointing out the latest developments. An overview of the timing signal reference model and of the stability quantities adopted in the new international standards was presented, and a standard practical measurement procedure was outlined. This measurement procedure has proven effective and very useful for gaining further insight into the actual performance

of telecommunications clocks and into some stability measurement issues. Several measurement results were provided to support the concepts with experimental evidence: the results shown represent a survey of the actual performance of clocks currently deployed in telecommunications networks.

ACKNOWLEDGMENT

The author would like to thank S. A. Dyer, the Acting Editor-in-Chief of this TRANSACTIONS, for his long and meticulous effort in reviewing this manuscript.

REFERENCES

[1] W. C. Lindsey, F. Ghazvinian, W. C. Hagmann, and K. Dessouky, "Network synchronization," *Proc. IEEE*, vol. 73, pp. 1445–1467, Oct. 1985.

[2] P. Kartaschoff, "Synchronization in digital communications networks," *Proc. IEEE*, vol. 79, pp. 1019–1028, July 1991.

[3] J. C. Bellamy, "Digital network synchronization," *IEEE Commun. Mag.*, vol. 33, pp. 70–83, Apr. 1995.

[4] "Digital hierarchy bit rates," ITU-T Rec. G.702, Blue Book, 1988.

[5] "Physical/electrical characteristics of hierarchical digital interfaces," ITU-T Rec. G.703, Blue Book, 1988.

[6] "Controlled slip rate objective on an international digital connection," ITU-T Rec. G.822, Blue Book, 1988.

[7] H. L. Hartmann and E. Steiner, "Synchronization techniques for digital networks," *IEEE J. Select. Areas Commun.*, vol. SAC-4, July 1986.

[8] "Network node interface for the synchronous digital hierarchy (SDH)," Geneva, ITU-T Revised Rec. G.707, Mar. 1996.

[9] "Definitions and terminology for synchronization networks," Geneva, ITU-T Rec. G.810, May 1996.

[10] "Timing characteristics of SDH equipment slave clocks (SEC)," Geneva, ITU-T Rec. G.813, May 1996.

[11] "Architecture of transport networks based on the synchronous digital hierarchy (SDH)," Geneva, §6, ITU-T Rec. G.803, Mar. 1993.

[12] "Generic requirements for synchronization networks," Bonn, ETSI Draft ETS 300 462, Sept. 1996.

[13] "Telecommunications synchronization interface standard," ANSI T1.101-1994.

[14] J. A. Barnes, A. R. Chi, L. S. Cutler, D. J. Healey, D. B. Leeson, T. E. McGunigal, J. A. Mullen, Jr., W. L. Smith, R. L. Sydnor, R. F. C. Vessot, and G. M. R. Winkler, "Characterization of frequency stability," *IEEE Trans. Instrum. Meas.*, vol. IM-20, May 1971.

[15] "IEEE standard definitions of physical quantities for fundamental frequency and time metrology," IEEE Std. 1139, approved Oct. 20, 1988.

[16] D. W. Allan, "Statistics of atomic frequency standards," *Proc. IEEE*, vol. 84, July 1996.

[17] L. S. Cutler and C. L. Searle, "Some aspects of the theory and measurement of frequency fluctuations in frequency standards," *Proc. IEEE*, vol. 84, Feb. 1996.

[18] P. Lesage and C. Audoin, "Characterization of frequency stability: Uncertainty due to the finite number of measurements," *IEEE Trans. Instrum. Meas.*, vol. IM-22, June 1973.

[19] W. C. Lindsey and C. M. Chie, "Theory of oscillator instability based upon structure functions," *Proc. IEEE*, vol. 64, Dec. 1976.

[20] P. Lesage and T. Ayi, "Characterization of frequency stability: Analysis of the modified Allan variance and properties of its estimate," *IEEE Trans. Instrum. Meas.*, vol. IM-33, Dec. 1984.

[21] L. G. Bernier, "Theoretical analysis of the modified Allan variance," in *Proc. 41st Annu. Frequency Control Symp.*, 1987.

[22] J. Rutman and F. L. Walls, "Characterization of frequency stability in precision frequency sources," *Proc. IEEE*, vol. 79, June 1991.

[23] P. Lesage and C. Audoin, "Characterization and measurement of time and frequency stability," *Radio Sci.*, vol. 14, no. 4, 1979, Amer. Geophysical Union.

[24] D. A. Howe, D. W. Allan, and J. A. Barnes, "Properties of signal sources and measurement methods," in *Proc. 35th Annu. Frequency Control Symp.*, 1981.

[25] S. R. Stein, "Frequency and time—Their measurement and characterization," in *Precision Frequency Control*, E. A. Gerber and A. Ballato, Eds. New York: Academic, 1985, vol. 2, ch. 2, pp. 191–232.

[26] F. L. Walls and D. W. Allan, "Measurement of frequency stability," *Proc. IEEE*, vol. 74, Jan. 1986.

[27] D. B. Sullivan, D. W. Allan, D. A. Howe, and F. L. Walls, Eds., "Characterization of clocks and oscillators," NIST Tech. Note 1337, Mar. 1990.

[28] D. W. Allan, "Time and frequency metrology: Current status and future considerations," in *Proc. 5th Eur. Frequency Time Forum*, 1991.

[29] F. L. Walls, A. J. D. Clements, C. M. Felton, M. A. Lombardi, and M. D. Vanek, "Extending the range and accuracy of phase noise measurements," in *Proc. 42th Annu. Frequency Control Symp.*, 1988.

[30] D. W. Allan and H. Daams, "Picoseconds time difference measurement system," in *Proc. 29th Annu. Frequency Control Symp.*, 1975.

[31] C. A. Greenhall, "A method for using a time interval counter to measure frequency stability," in *Proc. 41st Annu. Frequency Control Symp.*, 1987.

[32] C. Hackman and D. B. Sullivan, "Time and frequency measurement," *Amer. J. Phys.*, vol. 63, pp. 306–317, Apr. 1995.

[33] J. A. Barnes, "The measurement of linear frequency drift in oscillators," in *Proc. 15th Annu. Precise Time, Time Interval (PTTI) Meet.*, 1983.

[34] F. L. Walls and A. De Marchi, "RF spectrum of a signal after frequency multiplication: Measurement and comparison with a simple calculation," *IEEE Trans. Instrum. Meas.*, vol. IM-24, Sept. 1975.

[35] W. C. Lindsey and C. M. Chie, "A survey of digital phase-locked loops," *Proc. IEEE*, vol. 69, Apr. 1981.

[36] M. Carbonelli, D. De Seta, and D. Perucchini, "Characterization of timing signals and clocks," *Eur. Trans. Telecommun.*, vol. 7, Jan./Feb. 1996.

[37] S. Bregni, "Measurement of maximum time interval error for telecommunications clock stability characterization," *IEEE Trans. Instrum. Meas.*, vol. 45, Oct. 1996.

[38] V. F. Kroupa, "Noise properties of PLL systems," *IEEE Trans. Commun.*, vol. COM-30, Oct. 1982.

[39] S. Bregni, M. Carbonelli, D. De Seta, and D. Perucchini, "Impact of the time error sampling period on telecommunications clock stability measures," *Eur. Trans. Telecommun.*, vol. 8, pp. 573–582, Nov./Dec. 1997.

[40] S. Bregni and F. Setti, "Impact of the anti-aliasing pre-filtering on the measurement of maximum time interval error," in *Proc. IEEE GLOBECOM'97*, Phoenix, AZ, 1994.

[41] W. H. Press, B. P. Flannery, S. A. Teukolsky, and W. T. Vetterling, *Numerical Recipes in C: The Art of Scientific Computing*, 2nd ed. Cambridge, U.K.: Cambridge Univ. Press, 1992.

[42] S. Bregni, "AVAR, MAVAR, TVAR, TIErms measurement results on SDH equipment," Montpellier, ETSI TM3/WG6, TD no. 37, Feb. 1994.

[43] S. Bregni, M. Carbonelli, M. D'Agrosa, D. De Seta, and D. Perucchini, "Different behavior of frequency stability measures in independent and synchronized clocks: Theoretical analysis and measurement results," in *Proc. IEEE ICC'94*, New Orleans, LA, 1994.

Stefano Bregni (M'93) was born in Milano, Italy, in 1965. He received the Dott. Ing. degree in telecommunications engineering from the Politecnico di Milano and the M.Sc. degree from the CEFRIEL Centre, Milano.

In 1991, he joined SIRTI S.p.A., where he was mainly involved in SDH transmission system design and testing and network synchronization issues, with special regard to clock stability measurement techniques. Since 1994, he has been with CEFRIEL, where he is currently Head of the Transmission Systems Department.

Mr. Bregni has served on ETSI and ITU-T committees on digital network synchronization. He was Guest Editor of the *European Transactions on Telecommunications Focus on Synchronization of Digital Networks*.